

Crystallization kinetics with fragile-to-strong crossover in Zn-Sb-Te supercooled phase-change liquids

Cite as: Appl. Phys. Lett. **115**, 091903 (2019); <https://doi.org/10.1063/1.5116046>

Submitted: 21 June 2019 . Accepted: 13 August 2019 . Published Online: 27 August 2019

Jierong Gu, Yimin Chen , Qian Zhang, Guoxiang Wang , Rongping Wang , Xiang Shen, Junqiang Wang, and Tiefeng Xu



View Online



Export Citation



CrossMark

Applied Physics Letters

Mid-IR and THz frequency combs
special collection

Read Now!



Crystallization kinetics with fragile-to-strong crossover in Zn-Sb-Te supercooled phase-change liquids

Cite as: Appl. Phys. Lett. **115**, 091903 (2019); doi: 10.1063/1.5116046

Submitted: 21 June 2019 · Accepted: 13 August 2019 ·

Published Online: 27 August 2019



View Online



Export Citation



CrossMark

Jierong Gu,¹ Yimin Chen,^{1,2,a)} Qian Zhang,¹ Guoxiang Wang,¹ Rongping Wang,^{1,b)} Xiang Shen,^{1,c)} Junqiang Wang,^{3,4,d)} and Tiefeng Xu¹

AFFILIATIONS

¹Laboratory of Infrared Material and Devices & Key Laboratory of Photoelectric Materials and Devices of Zhejiang Province, Advanced Technology Research Institute, Ningbo University, Ningbo 315211, China

²Department of Microelectronic Science and Engineering, School of Physical Science and Technology, Ningbo University, Ningbo 315211, China

³CAS Key Laboratory of Magnetic Materials and Devices & Zhejiang Province Key Laboratory of Magnetic Materials and Application Technology, Ningbo Institute of Materials Technology & Engineering, Chinese Academy of Sciences, Ningbo 315201, China

⁴Center of Materials Science and Optoelectronics Engineering, University of Chinese Academy of Sciences, Beijing 100049, China

^{a)}chenyimin@nbu.edu.cn

^{b)}wangrongping@nbu.edu.cn

^{c)}shenxiang@nbu.edu.cn

^{d)}jqwang@nimte.ac.cn

ABSTRACT

Understanding crystallization kinetics is essential to select the high-performance materials for phase-change memory. By ultrafast differential scanning calorimetry, we found the distinct fragile-to-strong crossover crystallization kinetics in ZnSb and Zn₂₈Sb₅₄Te₁₈ supercooled liquids. Zn₂₈Sb₅₄Te₁₈ inherits the excellent thermal stability around glass transition from ZnSb and exhibits faster crystal growth rate close to melting temperature (U_{\max} is 9.1 m s^{-1}) and larger crossover magnitude f (2.3), compared to the typical fragile-to-strong crossover material Ag-In-Sb₂Te. Such a material with a distinct fragile-to-strong crossover is helpful to improve their thermal stability nearby glass transition temperature and accelerate the phase transition speed close to melting temperature.

Published under license by AIP Publishing. <https://doi.org/10.1063/1.5116046>

In order to respond to the explosive increase in information storage and processing, much research has been focused on the development of nonvolatile memory and neuroinspired computing technologies in recent decades.¹ Phase-change memory bases on chalcogenide materials, which are capable of switching rapidly and reversibly between amorphous and crystalline phases via an electric or optical pulse,² are leading candidates as the next nonvolatile memory. Recently, an artificial neuron has been reported that uses phase-change memory to realize an integrate-and-fire functionality with stochastic dynamics,³ and then weather data computing is realized by using an array of one million phase-change cells.⁴ The crystallization dynamics of a phase-change cell or a material was emphasized to reveal before realizing such neuroinspired data computing.⁵

The mechanism of the crystallization dynamics in phase-change materials has been discussed by studying the structural and kinetic experiments. The tool named ultrafast differential scanning calorimetry (DSC), which has fast scanning rate and high sensitivity, was performed to kinetics experiments in phase-change supercooled liquids (PCLs), such as Ge₂Sb₂Te₅ (GST),⁶ GeTe,⁷ and Ge₇Sb₉₃.⁸ Together with a suitable viscosity model, many important crystallization kinetic parameters, i.e., supercooled liquid fragility, temperature dependent viscosity, and crystal growth rate, have been deduced in such reports. Interestingly, Orava *et al.* found a fragile-to-strong crossover (FSC) in Ag-In-Sb₂Te (AIST) supercooled liquid using DSC and a generalized Mauro-Yue-Ellison-Gupta-Allan (g-MYEGA) viscosity model. Such FSC behavior was also discovered in Ge₁₅Te₈₅^{9,10} and ZnCl₂.¹¹ In PCLs, the FSC behavior supplies a chance to balance or alleviate the contradiction

between fast crystallization speed in high temperature that is close to T_m and a low crystal growth rate in low temperature that is nearby T_g . Undoubtedly, the behavior is helpful to accelerate amorphous-to-crystalline transition speed and improve amorphous thermal stability in a phase-change material. Recently, Chen *et al.* found that there is FSC behavior in GST and GeTe nanoparticles,^{12,13} which may be due to the dimensional limitation. It is believed that FSC appears to be widespread in glass-forming liquids¹⁴ and may also be a general feature in marginal glass-forming phase-change liquids.¹⁵ The key questions of FSC in PCLs are what is the degree of FSC (f) and at which temperature does FSC occur? It has been confirmed that the parameters of f and T_{f-s} can be tuned by doping in Cu-Zr-Al metallic glasses,¹⁶ and the tuning of the fragility of GST can be achieved by the addition of dopants, such as Al, Bi, C, and N.¹⁷ Moreover, it was reported that the temperature dependent crystal growth rate can change from a strong liquid to a weak liquid with an obvious non-Arrhenius behavior by increasing the Ge content in Ge-Sb PCLs.¹⁸ These results imply that the concept of tuning and finding the suitable T_{f-s} and high f value by doping or changing composition is significantly important in developing optimized phase-change materials for applications like the artificial phase-change neuron and so on.

In this work, we demonstrated an obvious FSC behavior in the ZnSb material, which was confirmed to have a good thermal stability and a reversible phase transition ability.¹⁹ However, it exhibits a relatively low crystallization speed in its supercooled liquid. Then, we designed a Sb-rich Zn-Sb-Te material, which is considered as a candidate for performance trade-off between crystallization speed and thermal stability² and confirmed that it has an FSC behavior with both ultrafast crystal growth rate in high temperature and very good thermal stability in low temperature.

Sb-rich Zn-Sb-Te films with a thickness of 300 nm were deposited on quartz and SiO₂/Si(100) substrates by magnetron cosputtering using different ZnSb and Sb₂Te alloy targets, and ZnSb films with the same thickness were grown by the sputtering method using a single ZnSb target. The base and working pressures were set to 2×10^{-4} and 0.35 Pa, respectively. The desired Zn₂₈Sb₅₄Te₁₈ (ZST) films were obtained by tuning the sputtering power at 30 W for the ZnSb target and at 50 W for the Sb₂Te target. The stoichiometry of these two films was examined by energy-dispersive spectroscopy. In order to obtain the specific temperature and latent heat for melting, ZnSb and ZST bulks were fabricated by the melt-quenching method, and about 10 mg material was sealed into an aluminum pan and tested by a conventional DSC (TA Q2000) with a heating rate of 10 K min⁻¹ in a nitrogen-protected ambient. Flash DSC 1 was employed to study the crystallization kinetics in ZnSb and ZST PCLs. The details of similar measurement processes, thermal lag estimations, temperature calibration, and Johnson-Mehl-Avrami (JMA) numerical simulations, were performed in the previous reports.^{7,20}

Figure 1(a) shows the ultrafast DSC traces of ZnSb. It can be seen that the peak temperature for crystallization (T_p) increases from 545 to 627 K with the increase in the heating rate from 10 to 40 000 K s⁻¹. Figure 1(b) shows the ultrafast DSC of ZST; the value of T_p increases from 548 to 593 K as the heating rate increases from 100 to 40 000 K s⁻¹. According to the JMA kinetic theory,²¹ we performed the numerical simulations of DSC traces for ZnSb and ZST, and the results are shown in Figs. 1(c) and 1(e), respectively. In Figs. 1(d) and 1(f), there is no significant difference in the value of T_p from the simulated and experimental DSC traces even at a high heating rate. Moreover, no obvious divergence

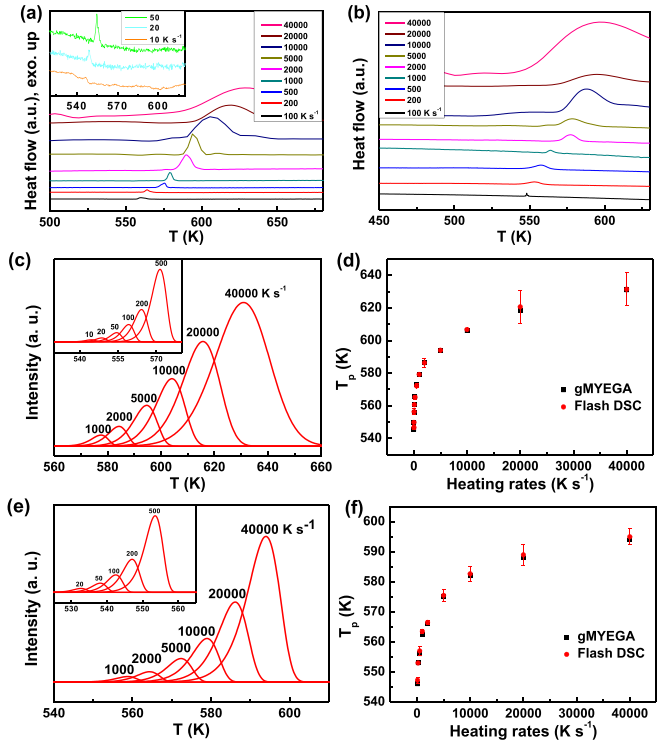


FIG. 1. (a) Ultrafast DSC traces for ZnSb at heating rates ranging from 10 to 40 000 K s⁻¹. (b) Ultrafast DSC traces for ZST at heating rates ranging from 100 to 40 000 K s⁻¹. (c) Numerical simulations of ZnSb DSC traces produced using the g-MYEGA model with heating rates ranging from 10 to 40 000 K s⁻¹. (d) Comparison of experimental and numerical T_p for ZnSb. (e) Numerical simulations of ZST DSC traces produced using the g-MYEGA model with heating rates ranging from 10 to 40 000 K s⁻¹. (f) Comparison of experimental and numerical T_p for ZST. The insets of (a), (c), and (e) show magnified images of the experimental and numerical DSC traces at low heating rates.

can be found between $T_{0.63}$ (the temperature at which the crystallized fraction is 0.63) and T_p as the heating rate is 40 000 K s⁻¹ and lower (details are not shown in here), indicating that the Kissinger method is a good approximation for crystalline growth.⁶ We thus carried out the Kissinger plots based on all T_p values obtained from ultrafast DSC and *in situ* sheet resistance test, and the results are shown in Fig. 2(a). The Kissinger method can be expressed as,²²

$$\ln(\phi/T_p^2) = -\frac{Q}{RT_p} + A, \quad (1)$$

where Q is the activation energy for crystallization, R is the gas constant ($R = 8.314$ J/mol/K), A is a constant, and ϕ is the heating rate. For these two plots, the Arrhenius behavior may be found in a low temperature range, but a non-Arrhenius behavior is obvious in a high temperature range. Thus, the g-MYEGA viscosity model was employed to describe it. That is²³

$$\log_{10}\eta = \log_{10}\eta(\infty) + \frac{1}{T \left[W_1 \exp\left(-\frac{C_1}{T}\right) + W_2 \exp\left(-\frac{C_2}{T}\right) \right]}, \quad (2)$$

where $\eta(\infty)$ is the viscosity at an infinite high temperature, W_1 and W_2 are the weight coefficients for describing the brittle phase and the

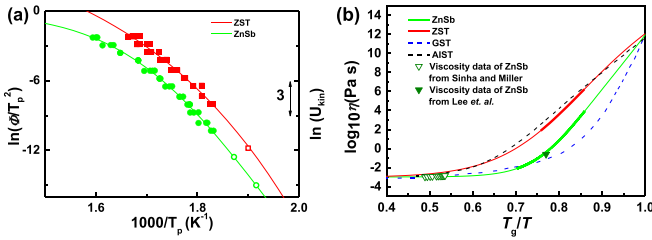


FIG. 2. (a) Kissinger plots for the crystallization of supercooled liquid ZST and ZnSb. The squares and spheres represent the experimental data from ultrafast DSC for ZnSb and ZST, respectively. The open square and circles are the data obtained from the test of sheet resistances as a function of temperature. The curves represent the crystallization kinetics U_{kin} , which are fitted by using the g-MYEGA viscosity model. (b) Angell plots for ZnSb and ZST. The T_g is set as the temperature where the viscosity is 10^{12} Pa s, which results in T_g being 445 K for ZnSb and T_g being 450 K for ZST. The thick regions represent the temperature region of ultrafast DSC data. The hollow and solid triangles represent the ZnSb viscosity data above T_m and nearby T_g from the references.^{24,25} Dashed blue and black curves are the Angell plots of GST and AIST obtained from Orava *et al.*^{6,15}

strong phase, and C_1 and C_2 are the two constraint starting temperature constants corresponding to the two mechanisms of brittleness and strength, respectively. Figure 2(b) exhibits the temperature dependent viscosity for ZnSb and ZST PCLs. The fitted parameters for ZnSb are $\log \eta(\infty) = -2.98 \pm 0.15$ Pa s, $W_1 = 848.3 \pm 42.4$ K⁻¹, $C_1 = 8397 \pm 420$ K, $W_2 = (1.56 \pm 0.078) \times 10^{-3}$ K⁻¹, and $C_2 = 1057 \pm 53$ K, with $R^2 = 0.994$. And, they are $\log \eta(\infty) = -3 \pm 0.27$ Pa s, $W_1 = 1.01 \pm 0.09$ K⁻¹, $C_1 = 4997 \pm 450$ K, $W_2 = 0.0036 \pm 0.0003$ K⁻¹, and $C_2 = 1573 \pm 142$ K, with $R^2 = 0.972$, for ZST. As we see, the fitted temperature dependent viscosities for ZnSb are all in good agreement with the reported viscosity data from Sinha and Miller (high temperature)²⁴ and Lee *et al.* (low temperature),²⁵ implying a validity of the FDSC method and g-MYEGA viscosity model used in this work.

A Stokes-Einstein relation is well accepted to describe the relationship between the crystallization kinetic coefficient U_{kin} and viscosity η as $U_{kin} \propto \eta^{-1}$.²⁶ In this work, therefore, the temperature dependence of U_{kin} can be written as

$$\log_{10} U_{kin} = C - \log_{10} \eta(\infty) - \frac{1}{T \left[W_1 \exp\left(-\frac{C_1}{T}\right) + W_2 \exp\left(-\frac{C_2}{T}\right) \right]}, \quad (3)$$

where C is a constant to indicate the difference between U_{kin} and η^{-1} . Together with the suitable C and the same fitting parameters employed before, the scattered dots in Fig. 2(a) can be fitted by using Eq. (3) to describe the temperature dependent U_{kin} as green and red curves for ZnSb and ZST, respectively.

The temperature dependence of the crystal growth rate can be described as²⁷

$$U = U_{kin} \left[1 - \exp\left(-\frac{\Delta G}{RT}\right) \right], \quad (4)$$

where U_{kin} is the crystallization kinetic coefficient as mentioned above, R is the gas constant, and ΔG is the Gibbs free energy. Following Thompson and Spaepen's suggestion,²⁷ the ΔG should be written as

$$\Delta G = \frac{\Delta H_m \Delta T}{T_m} \left(\frac{2T}{T_m + T} \right), \quad (5)$$

where ΔT is the undercooling temperature, ΔH_m is the latent heat of melting, and T_m is the melting temperature. By using the conventional DSC test, ΔH_m can be estimated as 1.225 and 16.2 kJ mol⁻¹ for ZnSb and ZST, and T_m is 774 and 830 K for ZnSb and ZST, respectively. Together with the same parameters employed before, we can thus estimate the temperature dependences of crystal growth rate for ZnSb and ZST PCLs, as described in Fig. 3.

As we see in Fig. 3, by using ultrafast DSC method, the crystal growth rate U from T_g to T_m can be detected, and the maximum growth rates U_{max} are readily observed as 0.01 and 9.1 m s⁻¹ for ZnSb and ZST, respectively. ZnSb was demonstrated to have an excellent thermal stability¹⁶ but moderate crystal growth rate, and thus it is not a good candidate for a high-speed phase-change application. However, a distinct FSC behavior was found in ZnSb PCLs; so, we designed the material of ZST, which may inherit good thermal stability from ZnSb and possess a fast crystal growth rate. Excitingly, the ZST PCL exhibits not only good thermal stability but also ultrafast crystallization speed. This is due to the distinct FSC behavior in ZST PCL, making it possible to combine low crystal growth rate nearby T_g and fast crystal growth rate close to T_m in one material.

The FSC behavior was first found in widely used oxide glasses, such as water²⁸ and SiO₂,²⁹ which was involved in the crystallization process and thermodynamic effects in their supercooled liquids. Such a behavior was demonstrated in metallic supercooled liquids like Cu-Zr¹⁶ and Al-Ni³⁰ based glasses, and it was suggested that it might be a general dynamic feature for all metallic supercooled liquids.²³ Ge₁₅Te₈₅^{31,32} and Ge₃₀Se₇₀^{33,34} as typical chalcogenide liquids were reported to have a distinct FSC behavior. For chalcogenide PCLs, it was confirmed that AIST has an FSC behavior with the viscosity crossover, as shown in Fig. 2(b). Another two conventional phase-change materials, GST and GeTe, were demonstrated to have no FSC behavior in their PCLs. However, Chen *et al.* reported that the FSC can be found in nanoparticles GST and GeTe.^{12,13} Orava *et al.* proposed that

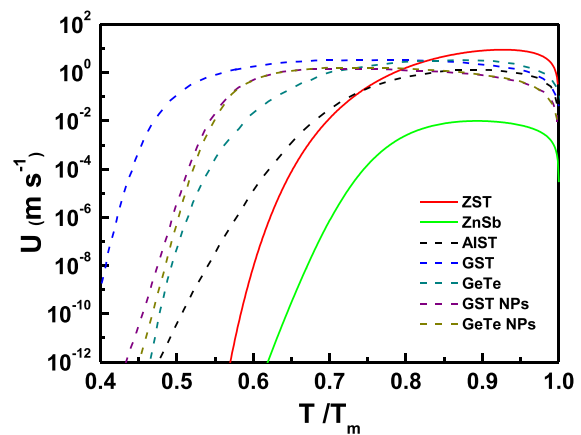


FIG. 3. The crystal growth rates of supercooled liquids of ZST and ZnSb as a function of temperature. These rates were calculated by using the g-MYEGA viscosity model. The dashed curves are the temperature dependent crystal growth rates for AIST,¹⁵ GST,⁶ GeTe,⁷ as well as the GST and GeTe nanoparticles (NPs).^{12,13}

the FSC may be a general feature for PCLs;¹⁵ so, it is key to know whether the FSC occurs in the supercooled temperature region (T_{f-s}) and how the crossover magnitude is (f).

The T_{f-s} can be calculated by the following equation:¹⁶

$$T_{f-s} = \frac{C_1 - C_2}{\ln W_1 - \ln W_2}. \quad (6)$$

They are 530 and 610 K for ZnSb and ZST PCLs, respectively, which are all higher than their T_g , suggesting these T_{f-s} values in the supercooled temperature region. We then used Angell's suggestion to estimate the fragility index.³⁵ Together with a plausible viscosity data at T_{f-s} , the fragility m and m' for strong and weak items can be defined as

$$m = \left[\partial \log_{10} \eta / \partial (T/T_g) \right]_{T=T_g}, \quad (7)$$

and

$$m' = \left[\partial \log_{10} \eta / \partial (T/T_g) \right]_{T=T_{f-s}}. \quad (8)$$

The values of m and m' are 60 and 91 for ZnSb, and they are 35 and 80 for ZST, respectively. Thus, the crossover magnitude f , which is defined as m'/m , can be estimated as 1.5 and 2.3 for ZnSb and ZST, respectively.

From the temperature dependent crystal growth rate, as shown in Fig. 3, we noted that the PCLs with an FSC behavior (besides of ZnSb) have both fast crystal growth rate close to T_m and low growth rate nearby T_g , especially for AIST and ZST. Compared to AIST, ZST has higher U_{\max} and lower crystal growth rate around T_g , indicating better data retention and faster switching capabilities for phase-change application. The phase-change materials with a high f value ($f > 2$) have the potential to solve the contradiction between ultrafast crystallization speed and good thermal stability. Hence, searching the phase-change material with a high f value is very beneficial for improving the performance of the integrated nonvolatile memory on the chip.

By using the ultrafast differential scanning calorimetry, we demonstrated a fragile-to-strong crossover in ZnSb supercooled liquid, which has an excellent thermal stability but a moderate phase transition speed, i.e., the maximum crystal growth rate U_{\max} is $\sim 0.01 \text{ m s}^{-1}$ at 690 K. Then, we designed a Sb-rich Zn-Sb-Te material, $\text{Zn}_{28}\text{Sb}_{54}\text{Te}_{18}$ (ZST), to inherit good thermal stability from ZnSb and fast crystallization speed from Sb_2Te . Interestingly, a fragile-to-strong crossover was also found in such Sb-rich phase-change supercooled liquid, which combines good thermal stability and fast crystallization speed in one material. Compared with the typical chalcogenide AIST PCLs that have an FSC behavior, ZST exhibits faster crystal growth rate close to T_m (U_{\max} is 9.1 m s^{-1} at $0.9 T_m$) and lower crystal growth rate around T_g (lower than $10^{-12} \text{ m s}^{-1}$), as well as the larger crossover magnitude f (2.3). The FSC behavior helps phase-change materials improve their data retention ability while increasing the crystallization speed. The concept of designing and tuning the crossover temperature T_{f-s} in the supercooled temperature region and obtaining a high crossover magnitude f can be important in developing optimized phase-change materials.

The project is supported by the National Natural Science Foundation of China (Grant Nos. 61775111, 61775109, 51771216, 61604083, 61904091), the Zhejiang Provincial Natural Science

Foundation of China (No. LR18E010002), the International Cooperation Project of Ningbo City (Grant No. 2017D10009), the One Hundred Talents Program of Chinese Academy of Sciences, and 3315 Innovation Team in Ningbo City and sponsored by K. C. Wong Magna Fund in Ningbo University, China.

REFERENCES

- W. Zhang, R. Mazzarello, M. Wuttig, and E. Ma, *Nat. Rev. Mater.* **4**, 150 (2019).
- Y. Chen, G. Wang, J. Li, X. Shen, T. Xu, R. Wang, Y. Lu, X. Wang, S. Dai, and Q. Nie, *Appl. Phys. Express* **7**, 105801 (2014).
- T. Tuma, A. Pantazi, M. Le Gallo, A. Sebastian, and E. Eleftheriou, *Nat. Nanotechnol.* **11**, 693 (2016).
- A. Sebastian, T. Tuma, N. Papandreou, M. Le Gallo, L. Kull, T. Parnell, and E. Eleftheriou, *Nat. Commun.* **8**, 1115 (2017).
- A. Sebastian, M. Le Gallo, and D. Krebs, *Nat. Commun.* **5**, 4314 (2014).
- J. Orava, A. L. Greer, B. Gholipour, D. W. Hewak, and C. E. Smith, *Nat. Mater.* **11**, 279 (2012).
- Y. Chen, G. Wang, L. Song, X. Shen, J. Wang, J. Huo, R. Wang, T. Xu, S. Dai, and Q. Nie, *Cryst. Growth. Des.* **17**, 3687 (2017).
- B. Chen, J. Momand, P. A. Vermeulen, and B. J. Kooi, *Cryst. Growth. Des.* **16**, 242 (2016).
- S. Wei, P. Lucas, and C. A. Angell, *J. Appl. Phys.* **118**, 034903 (2015).
- S. Wei, M. Stolpe, O. Gross, W. Hembree, S. Hechler, J. Bednarcik, R. Busch, and P. Lucas, *Acta Mater.* **129**, 259 (2017).
- P. Lucas, G. J. Coleman, M. Venkateswara Rao, A. N. Edwards, C. Devaadhithya, S. Wei, A. Q. Alsayoud, B. G. Potter, K. Muralidharan, and P. A. Deymier, *J. Phys. Chem. B* **121**, 11210 (2017).
- B. Chen, G. H. ten Brink, G. Palasantzas, and B. J. Kooi, *J. Phys. Chem. C* **121**, 8569 (2017).
- B. Chen, D. de Wal, G. H. Ten Brink, G. Palasantzas, and B. J. Kooi, *Cryst. Growth. Des.* **18**, 1041 (2018).
- F. Mallamace, C. Branca, C. Sarro, N. Leone, J. Spooren, S. H. Chen, and H. E. Stanley, *Proc. Natl. Acad. Sci. U. S. A.* **107**, 22457 (2010).
- J. Orava, D. W. Hewak, and A. L. Greer, *Adv. Funct. Mater.* **25**, 4851 (2015).
- C. Zhou, L. Hu, Q. Sun, H. Zheng, C. Zhang, and Y. Yue, *J. Chem. Phys.* **142**, 064508 (2015).
- J.-Y. Cho, D. Kim, Y.-J. Park, T.-Y. Yang, Y.-Y. Lee, and Y.-C. Joo, *Acta Mater.* **94**, 143 (2015).
- G. Eising, T. Van Damme, and B. J. Kooi, *Cryst. Growth. Des.* **14**, 3392 (2014).
- Y. Chen, G. Wang, X. Shen, T. Xu, R. P. Wang, L. Wu, Y. Lu, J. Li, S. Dai, and Q. Nie, *CrystEngComm* **16**, 757 (2014).
- Y. Chen, H. Pan, S. Mu, G. Wang, R. Wang, X. Shen, J. Wang, S. Dai, and T. Xu, *Acta Mater.* **164**, 473 (2019).
- M. Avrami, *J. Chem. Phys.* **9**, 177 (1941).
- H. E. Kissinger, *Anal. Chem.* **29**, 1702 (1957).
- C. Zhang, L. Hu, Y. Yue, and J. C. Mauro, *J. Chem. Phys.* **133**, 014508 (2010).
- A. Sinha and E. Miller, *Metall. Trans.* **1**, 1365 (1970).
- H. B. Lee, J. H. We, H. J. Yang, K. Kim, K. C. Choi, and B. J. Cho, *Thin Solid Films* **519**, 5441 (2011).
- Y. Chen, R. Wang, X. Shen, J. Wang, and T. Xu, *Cryst. Growth. Des.* **19**, 1103 (2019).
- C. V. Thompson and F. Spaepen, *Acta Metall.* **27**, 1855 (1979).
- C. Angell, *J. Phys. Chem.* **97**, 6339 (1993).
- I. Saika-Voivod, P. H. Poole, and F. Sciortino, *Nature* **412**, 514 (2001).
- Z. Chun-Zhi, H. Li-Na, B. Xiu-Fang, and Y. Yuan-Zheng, *Chin. Phys. Lett.* **27**, 116401 (2010).
- H. Neumann, F. Herwig, and W. Hoyer, *J. Non-Cryst. Solids* **205–207**, 438 (1996).
- J. Rocca, M. Erazu, M. Fontana, and B. Arcondo, *J. Non-Cryst. Solids* **355**, 2068 (2009).
- S. Stolen, T. Grande, and H.-B. Johnsen, *Phys. Chem. Chem. Phys.* **4**, 3396 (2002).
- Y. Gueguen, T. Rouxel, P. Gadaud, C. Bernard, V. Keryvin, and J.-C. Sangleboeuf, *Phys. Rev. B* **84**, 064201 (2011).
- C. A. Angell, *MRS. Bull.* **33**, 544 (2008).